Experimental Neurology 311 (2019) 148–161

Contents lists available at ScienceDirect

Experimental Neurology

journal homepage: www.elsevier.com/locate/yexnr

Research paper

Rapid plasticity of intact axons following a lesion to the visual pathways during early brain development is triggered by microglial activation

Luana da Silva Chagas[a], Pablo Trindade[c,d], Ana Lúcia Tavares Gomes[a], Henrique Rocha Mendonça[b], Paula Campello-Costa[a], Adriana da Cunha Faria Melibeu[a], Rafael Linden[b], Claudio Alberto Serfaty[a,e,*]

[a] Federal Fluminense University, Biology Institute, Neurobiology Department, Laboratory of Neural Plasticity – Niteroi, PO Box: 100180, Brazil
[b] Federal University of Rio de Janeiro, Biophisics Institute, Brazil
[c] D'Or Institute for Research and Education (IDOR), Rio de Janeiro, Brazil
[d] Post Graduating Program in Molecular and Cellular Biology, Federal University of the State of Rio de Janeiro, Brazil
[e] National Institute for Science and Technology in Neuroimmunomodulation – INCT/NIM, Brazil

ARTICLE INFO

Keywords:
Plasticity
Repair
Inflammation
Microglia
Axon sprouting
Monocular enucleation

ABSTRACT

Lesions in the central nervous system (CNS) can often induce structural reorganization within intact circuits of the brain. Several studies show advances in the understanding of mechanisms of brain plasticity and the role of the immune system activation. Microglia, a myeloid derived cell population colonizes the CNS during early phases of embryonic development. In the present study, we evaluated the role of microglial activation in the sprouting of intact axons following lesions of the visual pathways. We evaluated the temporal course of microglial activation in the superior colliculus following a contralateral monocular enucleation (ME) and the possible involvement of microglial cells in the plastic reorganization of the intact, uncrossed, retinotectal pathway from the remaining eye. Lister Hooded rats were enucleated at PND 10 and submitted to systemic treatment with inhibitors of microglial activation: cyclosporine A and minocycline. The use of neuroanatomical tracers allowed us to evaluate the time course of structural axonal plasticity. Immunofluorescence and western blot techniques were used to observe the expression of microglial marker, Iba-1 and the morphology of microglial cells. Following a ME, Iba-1 immunoreactivity showed a progressive increase of microglial activation in the contralateral SC at 24 h, peaking at 72 h after the lesion. Treatment with inhibitors of microglial activation blocked both the structural plasticity of intact uncrossed retinotectal axons and microglial activation as seen by the decrease of Iba-1 immunoreactivity. The local blockade of TNF-α with a neutralizing antibody was also able to block axonal plasticity of the intact eye following a ME. The data support the hypothesis that microglial activation is a necessary step for the regulation of neuroplasticity induced by lesions during early brain development.

1. Introduction

The assembly of functionally organized central connections in the mammalian brain occurs over a postnatal time window known as the critical period. This developmental period represents a stage where environmental clues promote a rapid use-dependent reorganization of neuronal networks, that under normal developmental conditions is required for the acquisition of proper sensory, motor and cognitive skills (Levelt and Hubener, 2012). As the critical period closes in primary sensory areas of the brain, such as visual, auditory, and somatosensory systems, a slow-down of use-dependent changes occurs resulting in more stable neural networks (Berardi et al., 2000). Plasticity and functional recovery is a rapid phenomenon after brain lesions in infants as compared to adult individuals (Mikellidou et al., 2017).

The subcortical visual system of rodents is a useful model for studying plasticity after partial brain lesions. During early postnatal development lesions such as a monocular eye enucleation or a restricted lesion to the contralateral retina trigger a series of adaptive responses from the intact eye's uncrossed retinocollicular pathway (Frost and Schneider, 1979; Hanson and Reese, 1993; Lund et al., 1980; Serfaty et al., 2005) resulting in extensive sprouting of axons from the intact eye over denervated territories (Godement et al., 1980; Reese, 1986;

* Corresponding author at: Instituto de Biologia, Universidade Federal Fluminense, Outeiro São João Batista s/n Centro, Niterói, Brazil.
E-mail address: cserfaty@id.uff.br (C.A. Serfaty).

https://doi.org/10.1016/j.expneurol.2018.10.002
Received 14 May 2018; Received in revised form 21 August 2018; Accepted 8 October 2018
Available online 09 October 2018
0014-4886/

Serfaty et al., 2005; Toldi et al., 1996). Indeed, it has been shown that retinal lesions during the critical period results in a rapid compensatory axonal sprouting of intact axons whereas the same lesion later on, after the closure of the critical period, results in a similar, but slower, plasticity time course (Serfaty et al., 2005).

After denervation, a rapid microglial activation occurs and precedes astrogliosis, mainly in contralateral but also in ipsilateral subcortical structures, including the lateral geniculate nucleus of the thalamus (dLGN) and superior colliculus (SC) (Gonzalez et al., 2006; Wilms and Bahr, 1995). In general, reactive glial cells are known to clean up axonal debris to restore tissue homeostasis and release growth factors and cytokines to stimulate neuronal sprouting (Bechmann and Nitsch, 1997). During early postnatal development microglial cells are actively involved in synaptic elimination and remodeling. In the adult CNS, microglia also promote active synaptic remodeling and plasticity. Decreased neuronal activity at synapses in both the developing and adult nervous system has been associated to physical removal of these less active connections (Wu et al., 2015). Despite great advances in the field, little is known about the sequence of events involved and the temporal correlation between microglial activation in a lesion environment and connectivity repair that might restore neural circuitry and function.

In the present study we studied the plastic response of intact axons to an early monocular enucleation, and the role and time course for microglial activation in this process. We aimed to study how a selective lesion recruits microglial activation and cytokine secretion and its temporal correlation to the compensatory axonal plasticity of intact axons in a model of monocular eye enucleation during the critical period of development. Understanding the mechanisms that allow a rapid plasticity during early brain development may be an important step to modulate plasticity and functional recovery in the adult central nervous system.

2. Materials & methods/methodology

2.1. Animals

All experiments were done with proper anesthesia to minimize any pain during manipulation and in strict accordance with The National Institutes of Health Guide for the Care and Use of Laboratory Animals. Experimental protocols were approved by the local Animal Care Committee (CEUA-UFF/ 0012009). Lister hooded rats at ages ranging from PND7 to PND17 were used for in vivo neuroanatomical, immunofluorescence and biochemical experiments. In one neuroanatomical experiment, the postlesion survival was extended to 1 year. Litters with no more than eight animals were maintained in a temperature- and humidity-controlled room under a 12 h light/dark cycle with free access to food and water.

2.2. Experimental design

2.2.1. Monocular enucleation

Under isoflurane anesthesia, a monocular eye enucleation was conducted at PND 10. Eye lids were opened, and after a quick dissection of extraocular muscles, the left eyeball was removed. A piece of gelfoam soaked in lidocaine was inserted into the orbit to promote local anesthesia. Palpebral borders were sutured with a cyanoacrylate gel. All animals were maintained at 37 °C and carefully monitored until full anesthetic recovery. During recovery animals were checked for any signs of discomfort and finally returned to their mother's cage.

2.2.2. Time course after monocular enucleation

Animals enucleated at PND10 were maintained for different survival times (Fig. 1). All groups were processed for HRP histochemistry or immunofluorescence and biochemical experiments for microglial detection.

2.2.3. Acute treatment

Three hours after a monocular enucleation experiment at PND10, animals were treated with a single subcutaneous injection of microglial blockers, either cyclosporine A (CsA - 50 mg/kg) or minocycline (125 mg/kg). The respective vehicles (DMSO 2% or PBS) were used as controls. Tissue processing occurred between 24 h and 1 year after the lesion for neuroanatomical, immunofluorescence and/or biochemical experiments.

2.2.4. Chronic treatment

One group of animals received a daily subcutaneous injections of cyclosporine A (CsA), 10 mg/kg from PND7 to PND10, while the control group was treated with vehicle (DMSO). At PND10, animals were enucleated, and processed 24 h after the induced lesion.

2.2.5. Local delivery of neutralizing antibody

To evaluate a role for TNF-α in the sprouting of intact axons from the non-lesioned eye, a local delivery of a neutralizing anti-TNF-α antibody (5 μg/μl, Cell Signaling) was performed through subpial implants of ethylene vinyl acetate polymer (Elvax®, Dupont) loaded with nTNF-α at PND7 (Fig. 1). At PND 10, animals received a monocular enucleation and tissue processing occurred 24 h after the lesion. A non-lesioned group received the same nTNF-α neutralizing antibody in ELVAX® as a control.

2.3. Anterograde tracing of retinocollicular projections

At the appropriate time window (Fig. 1), the uncrossed retinocollicular projection was traced by an intravitreal injection of a 30% horseradish peroxidase (HRP type VI, Sigma) solution in 2% dimethylsulphoxide (DMSO) in 0.9% NaCl into the vitreous chamber of right eye. After 24 h, the animals were deeply anaesthetized with isoflurane and perfused through the heart with saline (0.9% NaCl) containing 0.1% heparin followed by a mixture of aldehydes (1% paraformaldehyde and 2% glutaraldehyde) in 0.1 M phosphate buffer (pH = 7.4). The brains were removed, cryoprotected (20% sucrose in the same buffer) and coronal brain sections (40 μm) were processed for HRP histochemistry (Mesulam, 1978). This method provides a high sensitivity and stability of axon and terminal labeling, ideal for the study of the uncrossed retinofugal axonal population after a bulk intravitreal injection of the tracer (Oliveira-Silva et al., 2007; Serfaty et al., 2005; Trindade et al., 2011). Sections of the ipsilateral superior colliculus were visualized using dark-field optics with polarization filters in a Leica DM 2500 microscope under 100× magnification and images were obtained with a digital camera mounted on the microscope stage. For all experimental groups, the axonal terminal labeling of the contralateral SC was examined and taken as an internal control for homogeneous tracer uptake, transport, histochemical labeling or the occurrence of any accidental lesion during intraocular tracer delivery. The uncrossed (intact) pathway was analyzed in five sequential sections centered at the peak density of terminal labeling of the ipsilateral retinocollicular terminal fields, at the mid-rostral half of the superior colliculus (Serfaty and Linden, 1991). This region is, therefore, correspondent to the region where ipsilateral fibers normally branch and converge into clusters of terminals at the ventral portion of *stratum griseum superficiale* (SGS). We performed two types of densitometric analyses: a Global Visual Layer densitometry (SGS and *stratum zonale*) and a more specific Dorsal Layer Densitometry (upper SGS and *stratum zonale*), where most of plasticity is expected to occur (Supplementary Fig. 1). Pixel densities were measured on a 0–255 scale, in which 255 corresponded to white. Mean pixel values, measured with ImageJ™ 1.49 software, were obtained in the visual layers of the SC and subtracted from background densities measured in deep, non-visual layers in every section.

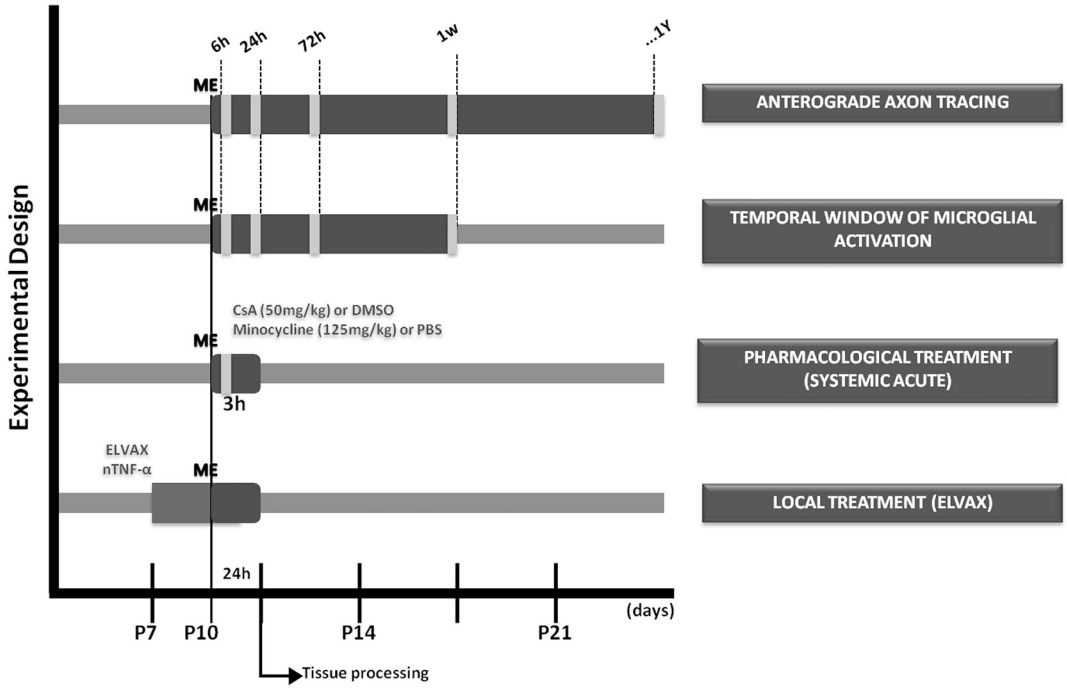

Fig. 1. Temporal scheme of experimental groups.

2.4. Immunofluorescence imaging

Animals ranging from PND10 to PND17 were deeply anaesthetized with isoflurane before a trans cardiac perfusion with saline (NaCl 0.9%) containing 0.1% heparin followed by a 4% paraformaldehyde solution in 0.1 M phosphate buffer (PBS), pH = 7.4, for 20 min. After brain removal and cryoprotection, 10 µm thick coronal sections were cut in a cryostat and mounted on gelatinized slides. Sections were washed in 0.1 M PBS, pH 7.4 and blocked in 10% normal goat serum (NGS) in the same buffer plus Triton-X 0,2% (PBS-T) for the next two hours. Sections were then incubated overnight with the primary antibody (1:1000 anti-Iba-1, Wako®; 1:10000 anti-CaN, Sigma®) diluted in PBS-T containing 5% NGS. After several washes in PBS, the sections were incubated either in AlexaFluor488/594-conjugated anti-rabbit (1:1000, Invitrogen®) or anti-mouse (1:200, Invitrogen®) secondary antibodies for 2 h. Images from the visual layers of the SC were acquired using a Leica DM 5500B deconvolution microscope under 400× magnification. Densities of total Iba-1 positive and ameboid-like Iba-1 positive immunoreactivity were obtained in the superficial layers of the colliculus contralateral to the monocular enucleation (ENU SC). The colliculus ipsilateral to enucleation (which received a minor deafferentation) was taken as an internal control (CT SC). Cell counts were performed taking sections from the rostral half of the SC where the uncrossed pathway in pigmented rats has its maximum density (Serfaty and Linden, 1991).

2.5. Quantification of ameboid microglial cells

Quantitative analysis was done by counting anti-Iba-1 immunoreactive cells in photomontages of the superior colliculus. The selection criteria for cell reactivity was based on morphological aspects and fluorescence intensity. Amoeboid, “reactive” cells, were characterized with large, rounded and highly immunolabeled cell bodies associated with few and short processes. We also analyzed the total number of Iba-1 + cells, where we included ameboid, reactive cells as well as ramified cells with long branches and low fluorescence intensity. The number of cells was normalized against the area of the entire section of the SC. Mean values were obtained from at least 3 coronal sections of each animal analyzed, considering at least 3 different animals for each group. All cell counts were done blind.

2.6. Western blot

Superior colliculi of animals ranging from PND10 to PND17 were dissected and homogenized in ice-cold RIPA buffer. Protein concentration analysis was carried out through Bradford method and their final concentrations were normalized with a lysis buffer containing 0.1% SDS. Samples (30 µg protein/lane) were separated by SDS/PAGE (15% concentrating gel) and electrotransferred to PVDF membranes (Amersham Biosciences®). Unspecific sites were blocked for 2 h at room temperature with 5% non-fat milk in Tris-buffered saline containing 0.1% Tween 20 (TBS-T pH 7.6). Membranes were, then, incubated overnight at 4 °C with rabbit anti-Iba-1 (1:750, Wako®), rabbit anti-total Erk (1:1000, Santa Cruz®), mouse anti b-tubulin (1:1000 Millipore) primary antibodies. Next, membranes were incubated with secondary HRP-conjugated antibodies (donkey anti-rabbit, 1:5000; from Biorad®) in TBS-T for 1 h. Then, membranes were revealed using Luminata™ Western Chemiluminescent HRP Substrates (Millipore®). All the membranes were re-probed for total Erk or b-tubulin immunoreactivity to confirm that similar amounts of protein were applied into gels. The detection of chemiluminescence was performed using a ChemiExpress system (Loccus Biotecnlogia®) and the densitometry analysis by ImageJ™ software.

2.7. Local TNF-α Inhibition in vivo

Elvax® polymers were used for local, in vivo, delivery of neutralizing anti-TNF-α antibodies. Elvax® was prepared accordingly, as previously described (Smith et al., 1995; Trindade et al., 2011). The loading concentration of drugs in Elvax® polymers is usually 100–1000-fold the concentration used for in vitro studies due to the slow kinetics of drug release in Elvax® (Smith et al., 1995). Briefly, Elvax® beads were washed in 95% alcohol for 1 week and then dissolved in dichloromethane (100 mg Elvax®/ml). Next, PBS (vehicle) or neutralizing anti-TNF antibody (5 µg/µl, Cell Signaling) were added to Elvax® solution followed by the addition of Fast green, 0.01% to aid Elvax® slice visualization. The final mixture was vortexed, rapidly frozen in dry ice/

acetone bath and stored for at least 7 days at -20 °C. Afterwards, the frozen mixture was lyophilized under mild vacuum at -20 °C for 24 h to remove water and solvent. Thereafter, 120-μm-thick slices were obtained using a cryostat. The animals submitted to Elvax® implants (at PND 7) had their skull and underlying dura mater cut and the surface of the midbrain exposed, under anesthesia with isoflurane. Elvax® slices were carefully placed over the SC, the bone fragment replaced, and the skin sutured with a thin layer of cyanoacrylate gel. Animal's recovery was monitored while they were kept at 37 °C, before returning to their cages.

2.8. Statistical analysis

The statistical analysis and graphs were plotted using GraphPad Prism 5.0 software (GraphPad Software, Inc. San Diego, CA, USA). Comparisons between two groups were performed using Student's unpaired *t*-test and for more than two groups we performed using ANOVA with Dunnett post-test. For all analyses, the data were shown as mean and standard error of the mean (SEM). Differences were considered significant when $p < .05$.

3. Results

3.1. Temporal window of structural plasticity of intact axons following a monocular enucleation at PND10

In the present study, we studied the time course of plasticity of intact retinal axons following a lesion to the contralateral pathway during early postnatal development (PND10). As shown in previous studies (Serfaty et al., 2005; Serfaty and Linden, 1994), at PND10, the ipsilateral retinocollicular projection has already developed adult-like clusters of terminals, mostly on the ventral border of the collicullar visual layers (*stratum griseum superficiale* - SGS) (Fig. 2A). Following a monocular enucleation of the contralateral eye, the anterograde tracing of the intact, ipsilateral pathway from the remaining eye showed a significant increase in axon and terminal labeling throughout the visual layers of the SC with a robust sprouting oriented to the dorsal SGS/SZ, starting after 6 h (Fig. 2B) and peaking at 24 h after a ME (Fig. 2C). This rapid plasticity was maintained at 72 h and 7 days post lesion (Fig. 2D, E) and was stable even after a one-year survival (Fig. 2F).

The global densitometric analysis of terminal labeling in the visual layers of the superior colliculus showed a significant increase (over 200%) of the experimental groups, except for the 6 h postlesion survival group, (Fig. 2G) and over an 800% increase in the densitometric analysis of upper dorsal layers (Fig. 2H). Together, these data suggest a fast and intense adaptive plasticity of intact axons in response to a lesion early in development that remains stable for long period of time.

3.2. Time-course of microglial reactivity after monocular enucleation

To evaluate changes on microglial profiles after a monocular enucleation at PND10 we performed immunohistochemical experiments for Iba-1 immunostaining in the contralateral SC contralateral at specific time intervals. Thus, enucleated animals were studied at 6 h, 24 h, 72 h and 7d post lesion. The colliculus ipsilateral to a ME was taken as an internal control. In normal, non-enucleated PND 10 animals, we observed few Iba-1 positive cells with ramified phenotype sparsely distributed through the visual layers of the SC (Fig. 3A, B). Six hours following a ME, no significant morphological changes were observed between the control and deafferented sides of the SC (Fig. 3C, D). However, 24 h after a ME, the right colliculus, contralateral to a ME (ENU) showed a robust increase in IBA-1 profiles invading the upper collicular visual layers with an evident redistribution of amoeboid microglial profiles, with short filaments and large rounded cell bodies (Fig. 3F) as compared both to a non-lesioned PND10 control and also to the non-enucleated (left) colliculus used as an internal control (CT) (Fig. 3E). An increase in Iba-1 positive cells, heterogeneously distributed throughout the ENU SC was also observed at 72 h post lesion although with decreased amoeboid and increased ramified profiles (Fig. 3G, H). One week after the lesion, Iba-1 immunoreactivity returned to base line values, similar to that observed in non-lesioned groups at PND10 with no evident morphological change when compared to its internal control (Fig. 3I, J). Quantitative analyses showed that total number of Iba1 positive cells do not vary significantly in experimental groups (Fig. 3L). However, quantification of reactive microglial cells showed a 2.9 fold increase 24 h after the lesion. A smaller, but noticeable increase of reactive microglia is still observed 72 h after monocular enucleation. Seven days after a ME, Iba-1 + cells are still present in both colliculus, but amoeboid cells are reduced nearly to control, non-enucleated levels (Fig. 3M). Western blot analysis taken of samples including both visual and non-visual collicular layers showed no significant increase in total Iba1 content at 24 h post lesion. However, Iba1 content showed an 80% increase 72 h after ME in the contralateral SC (Fig. 3N) when compared to the control side (ipsilateral to a ME) (Fig. 3O).

3.3. An acute systemic treatment with CsA inhibits plasticity and microglial reactivity induced by monocular enucleation at PND10

Calcineurin has a classical role on immunological activation, through the Ca2 + -CaN-NFAT pathway, including microglial activation (Nagamoto-Combs and Combs, 2010; Shiratori et al., 2010). Thus, to investigate the role of microglial activation in the induction of axonal sprouting induced by ME, we performed a single-dose/acute treatment with CsA (cyclosporine A, 50 mg/kg), 3 h after a ME at PND10 (Fig. 1). Vehicle treated animals given a ME showed an overall expansion of axonal terminal labeling both in the ventral border of the stratum griseum superficiale (SGS) and in axonal terminals sprouting toward the superficial aspects of the SGS (upper SGS) (Fig. 4A). On the other hand, a single dose of CsA resulted in reduced density of terminal and axonal anterograde labeling throughout the SC, showing that axons from the intact eye did not display a normal reactive plasticity present in the control group (Fig. 4B). Quantitative densitometric analyses showed a 46,5% decrease of the axonal density in the visual layers (Fig. 4C) and a 44,2% decrease of specific dorsal aspects of the SGS (Fig. 4D) as compared to the vehicle treated group. Therefore, we tested whether Cyclosporine A, could also affect microglial activation in immunohistochemical experiments. The deafferented (ENU) SC of vehicle-treated enucleated animals showed an increase in microglial cells, most of which displaying an amoeboid profile most of it in the upper visual layers (SGS) (Fig. 5B), as compared to the control (CT) side (Fig. 5A). On the other hand, the CsA treated group showed a marked reduction in IBA-1 amoeboid phenotype with most of cells presenting a ramified phenotype as compared to the vehicle treated group (Fig. 5D). Quantitative analysis of Iba-1 amoeboid cells in both vehicle and CsA groups, showed that ME induced in the contralateral SC a 4,3-fold increase of amoeboid cells in vehicle (DMSO) group and a 4-fold increase on CsA group, when compared to the respective internal controls, as expected. However, CsA treatment induced a 48,9% reduction in amoeboid microglia in deafferented (ENU) SC when compared to the control, vehicle-treated group (Fig. 5F). Interestingly, no difference was observed in the number of total microglial cells between all groups, suggesting a redistribution in microglial phenotypes after an acute lesion (Fig. 5E). Similar results were obtained with a chronic CsA systemic treatment (10 mg/kg, daily sc injections) from PND 7–10. We found a lack of plasticity and a similar reduction in reactive microglial cells within the collicular visual layers (Supplementary Fig. 2).

To confirm if calcineurin in fact mediates microglial reactivity in lesion conditions, we performed a co-localization experiment using CaN and Iba-1 markers. Indeed, we observed a strict co-localization of CaN on amoeboid microglia phenotype, 24 h after a ME at PN10 (Fig. 5I). Taking together, these data suggests that a CsA decreases plasticity

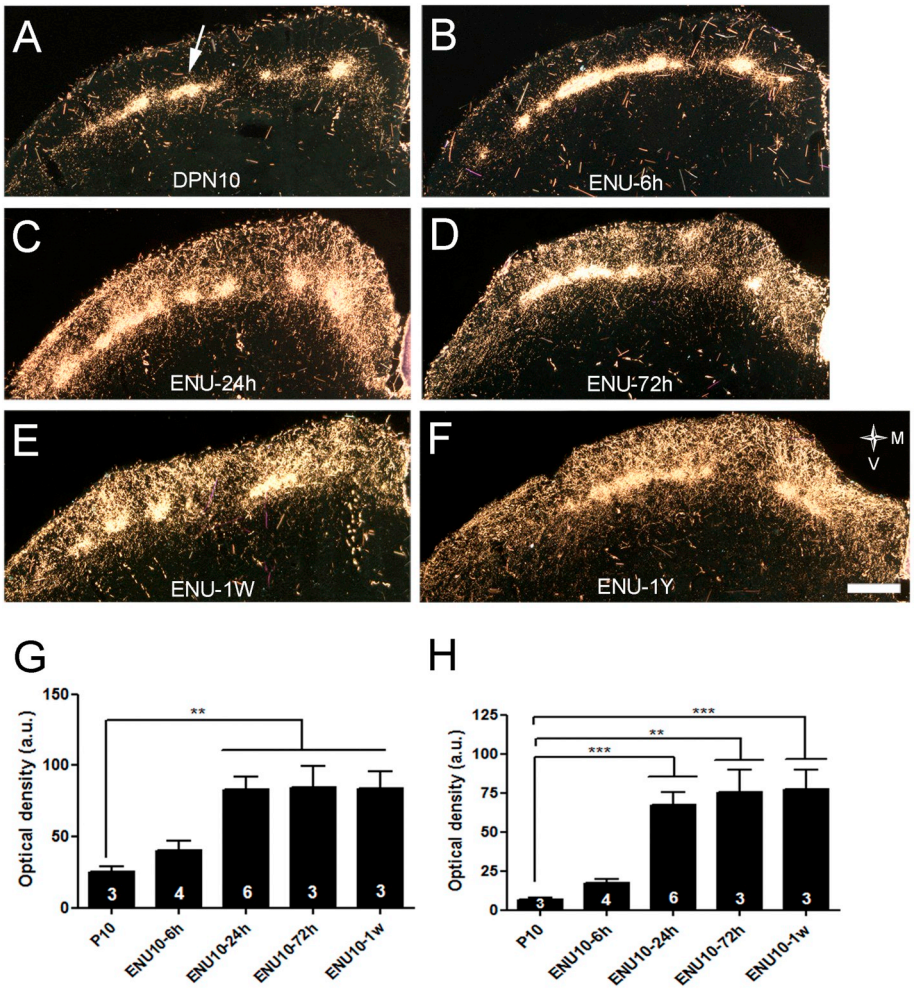

Fig. 2. Time course of plasticity of intact ipsilateral retinocollicular axons induced by a monocular enucleation at PND10. Dark-field photomicrographs of coronal sections of the rostral superior colliculus illustrate the reactive spouting of the ipsilateral pathway induced by a monocular enucleation (contralateral side) at PND10 at different survival times. (a) At PND 10, the uncrossed pathway of control, non-lesioned animals, display a normal pattern of axonal terminal labeling distributed in discrete clusters along the ventral border of the collicular visual layers (arrow). (b) 6 h after a contralateral ME, the uncrossed pathway from the intact eye displays a near to normal terminal field distribution. (c) 24 h after a ME, a robust sprouting of the uncrossed retinocollicular axon terminals is observed throughout the collicular visual layers. The sprouting remains unchanged at 72 h (d), 1 week (e) and 1 year (f) after the lesion. Quantification of the mean optical densities of the total collicular visual layers (g,) and the dorsal SGS (h) revealed significant differences that confirm the sprouting of retinocollicular fibers 24 h after a monocular enucleation at PND10.; ANOVA, post-hoc Tukey. * = $p < 0,05$; ** = $p < 0,01$; *** = $p < 0,001$. n of each group is expressed on bars. In photomicrographs, M indicates medial; V, ventral. Scale bar marks 200 μm.

through the inhibition of calcineurin and the blockade of microglial reactivity.

3.4. Acute systemic treatment with Minocycline inhibits plasticity and microglial reactivity induced by monocular enucleation at PND10

Since CaN has functions and targets in the CNS independent of its role on microglial reactivity, such as the modulation of synaptic plasticity and long term depression (LTD) (Baumgartel et al., 2008; Mulkey et al., 1994), we tested whether minocycline, a well described suppressor of microglial activation and neuroinflammation (Henry et al., 2008; Zheng et al., 2015) could also inhibit both plasticity and microglial activation. Acute systemic minocycline treatment (125 mg/kg, sc), delivered 3 h after a ME at PND10, was able to inhibit the axonal sprouting of the intact ipsilateral retinal axons 24 h post-lesion (Fig. 6B) when compared to a vehicle treated control group (Fig. 6A). Quantitative densitometric analysis showed a 50,5% reduction in axon density into the collicular visual layers (Fig. 6C) and 48,6% decrease of dorsal layers of SC in the minocycline-treated group when compared to the PBS group (Fig. 6D).

IBA-1 Microglial immunofluorescence showed an expected increase in microglial cells displaying an amoeboid profile in the deafferented (ENU) SC of vehicle-treated group (Fig. 7B). Minocycline treatment promoted a 31% reduction in Iba-1 amoeboid phenotype (Fig. 7F), with the prevalence of cells presenting a ramified phenotype as compared to the vehicle treated group, most of which in the upper visual layers of SC (Fig. 7D). In both vehicle and minocycline groups, we observed lesion-specific effects on microglial reactivity in the denervated SC when compared to the respective internal controls (Fig. 7 A, C): a 3.2 fold increase of amoeboid cells in PBS group and a 2.4 fold increase on Minocycline group (Fig. 7F). Like the CsA acute treatment, minocycline did not interfere with the number of total microglia, only preventing the appearance of amoeboid phenotype (Fig. 7E). Taken together, these results endorsed a role for reactive microglia in triggering structural neuroplasticity induced by a ME during early postnatal development – the critical period.

To investigate if an acute treatment with CsA or minocycline would lead to a permanent blockade in plasticity we tested a long-term survival (7 days) experiment following an acute treatment 3 h after lesion at PND10. The results revealed no inhibitory effects of both treatments over axon sprouting to the dorsal layers of the SC (Supplementary Fig. 4) showing a transitory effect of these treatments over structural plasticity. This also points that the results above described are not due neurotoxic effects upon nervous cells, once we observe the recurrence of axonal sprouting.

The pharmacological inhibition of microglial activation was confirmed by western blot experiments. We analyzed total Iba-1 content in visual and non-visual layers of the SC after the acute treatments with either CsA or minocyline and compared with vehicle-treated control groups. The colliculus ipsilateral to eye enucleation was used as an internal control. Although no difference has been found 24 h after eye enucleation (Supplementary Fig. 3), a robust inhibitory response was observed in the SC contralateral to enucleation 72 h after the lesion: a significant 50% decrease of Iba-1 content was found in the CsA group (single dose, 3 h after ME). Also, a 58.6% inhibition of Iba-1 increase was found in enucleated animals treated with minocycline in the same

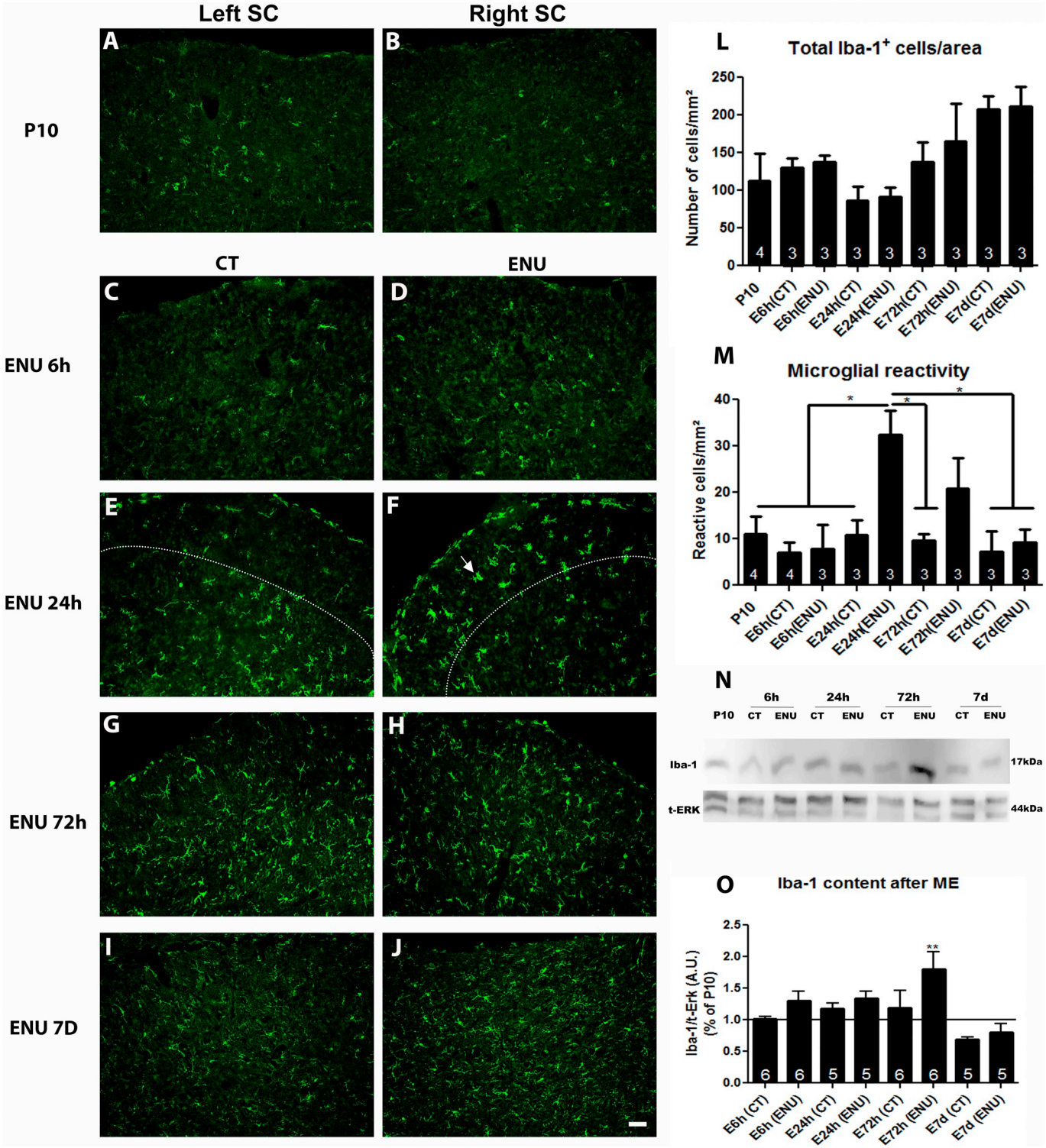

Fig. 3. Time-course of microglial reactivity in the SC after a monocular enucleation at PND10. No difference is noticed in Iba-1 immunoreactivity between the right (a) and left (b) SC of a non-enucleated PND10 animal. Iba-1 immunoreactivity of enucleated animals at PND10 within 6 h (c, d); 24 h (e, f); 72 h (g, h) and 7d (i, j) survival time. Panels d, f, h, and j represent the SC contralateral to a ME (ENU side), thus displaying a maximum denervation, while panels c, e, g and i represent internal controls showing the SC ipsilateral to a ME (CT side), thus displaying a minimum denervation. Notice the progressive increase of Iba-1 immunoreactivity on the ENU SC over time. An increase of amoeboid microglia phenotype is evident 24 h after monocular enucleation (f, arrow), specially on the upper visual layers of the SC (dashed line). An overall increase on the number of Iba-1 + cells colonizing the SC is observed 72 h after the lesion (h). Cells counts of the total number of Iba-1 + cells showed no significative differences (i) while the quantification of reactive cells revealed significant differences between ENU and CT sides of the SC 24 h after a ME (m). ANOVA, post-hoc Tukey analysis; * = $p < 0,05$. Western blot analysis of Iba-1 content in non-lesioned colliculi as well as in the ENU and CT sides of enucleated animal at PND10 (n). A band of 17 kDa shows a great increase on ENU 72 h group. (o) ANOVA, post-hoc Dunnett's revealed significant differences for Iba-1 expression 72 h after ME when compared to the non-lesioned PND10 animal, used as a control group. The n of each group is expressed on bars. Quantification was obtained by at least 3 different experiments for each group. * = $p < 0,05$; ** = $p < 0,01$; *** = $p < 0,001$. In photomicrographs the scale bar marks 50 μm.

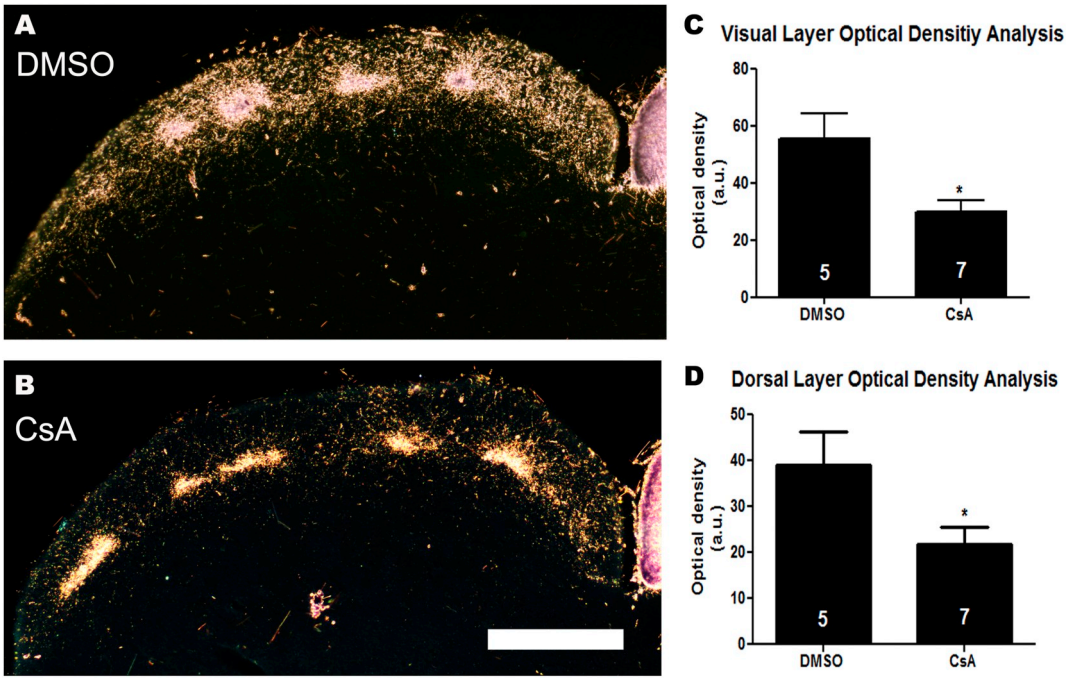

Fig. 4. Acute systemic treatment with CsA blocks axon plasticity of the intact ipsilateral pathway induced by a monocular enucleation at PND10. Dark-field photomicrographs of coronal sections of the ipsilateral retinocollicular pathway labeled with HRP. Axonal distribution of ipsilateral axons in vehicle-treated (DMSO) animals 24 h after a monocular enucleation of the contralateral eye reveals a sprouting of the intact pathway throughout the collicular visual layers (a). However, the systemic treatment with CsA completely inhibits axonal plasticity under the same lesion condition (b). The mean optical density of both the total collicular visual layers (c) or dorsal SGS (d) confirm the reduction of plasticity after an acute CsA treatment in enucleated animals. Quantification was obtained by at least 3 different experiments for each group. The n of each group is expressed on bars. Unpaired student's *t*-test analysis * = $p < 0,05$; ** = $p < 0,01$; *** = $p < 0,001$. In photomicrographs the scale bar marks 200 μm.

time interval. (Fig. 8).

3.5. Local treatment with neutralizing TNF-α antibody prevents plasticity induced by monocular enucleation at PND10

Lesions to the CNS promote the release of a variety of proinflammatory cytokines by microglia and astrocytes. TNF-α, has been implicated a dual role depending on the lesion context, through different signaling pathways. To investigate possible mechanisms that could mediate microglial activation and the release of TNF-α on plasticity induced by ME we used a local implant of Elvax® loaded with a neutralizing anti-TNF-α antibody implanted over the SC at PND7. We observed the impact on the plasticity of intact axons induced by ME at PND10, 24 h after the lesion. Local treatment with neutralizing TNF-α antibody abolished the plastic reorganization of the intact ipsilateral retinal axons after a ME (Fig. 9C) when compared to a vehicle treated control (Fig. 9A). Quantitative densitometric analyses showed a 59,4% reduction in the optic density of axonal retinal labeling into the collicular visual layers on the nTNF-α group when compared with PBS enucleated group (Fig. 9D). To control for unspecific effects of the neutralizing antibody, the same treatment was done in non-lesioned animals (Fig. 9B). Indeed, no difference in the distribution of terminal labeling was observed in this group as compared to a normal non-lesioned, non-treated group (Fig. 2A). No difference was observed when the ENU group treated with nTNF-α (Fig. 9C) was compared with a non-lesioned control group that also received nTNF-α (Fig. 9B, D).

4. Discussion

Although, many studies have focused on a role for microglial cells on the mechanisms associated with a normal developmental plasticity, such as synaptic pruning (Kaur et al., 2017; Wu et al., 2015), little is known on the influence of activated microglia and the critical mechanisms mediating a reactive plasticity of non-lesioned neurons and its axonal pathways. In the present study, we analyzed the role of microglia, in the plasticity induced by monocular enucleation. We used the rodent retinocollicular projections to describe that microglial activation induced by a massive neuronal denervation is required for a rapid axonal sprouting of intact converging pathways in the visual system. We also demonstrate that such regenerative response is markedly blocked by immunosuppressant drugs. We showed that 1) a marked plasticity of the ipsilateral, non-lesioned retinocollicular axons, is observed in the visual layers of the SC 24 h after lesion that strictly correlates with a peak of amoeboid microglial phenotype, observed 24 h after a ME; 2) after a lesion, microglial cells express CaN and its inhibition with CsA or minocycline decreases the axonal sprouting induced by a ME; 3) Also, CsA of minocycline reduce microglial activation in the collicular visual layers in the same time course 4) TNF-alfa is necessary for plasticity of intact axons in response to a central lesion. Collectively, our data suggest that microglia activation and inflammation is a key player in lesion-induced plasticity in the rodent retinotectal circuitry during early development and may account for the rapid plasticity observed during a developmental critical period in infants.

4.1. Monocular enucleation as a model for plasticity of intact axonal pathways

Monocular enucleation is considered a valuable tool to study different aspects of visual, cross-modal and developmental plasticity in the mammalian visual system (Nys et al., 2014; Steeves et al., 2008; Toldi et al., 1996; Van Brussel et al., 2011). Monocular enucleation (Lund et al., 1980; Nys et al., 2015) and restricted retinal lesions (Serfaty et al., 2005) have been used as a model of lesion-induced plasticity in the visual system revealing critical periods of development of subcortical visual pathways (Serfaty et al., 2005).

The removal of one eye results in massive denervation of retinal

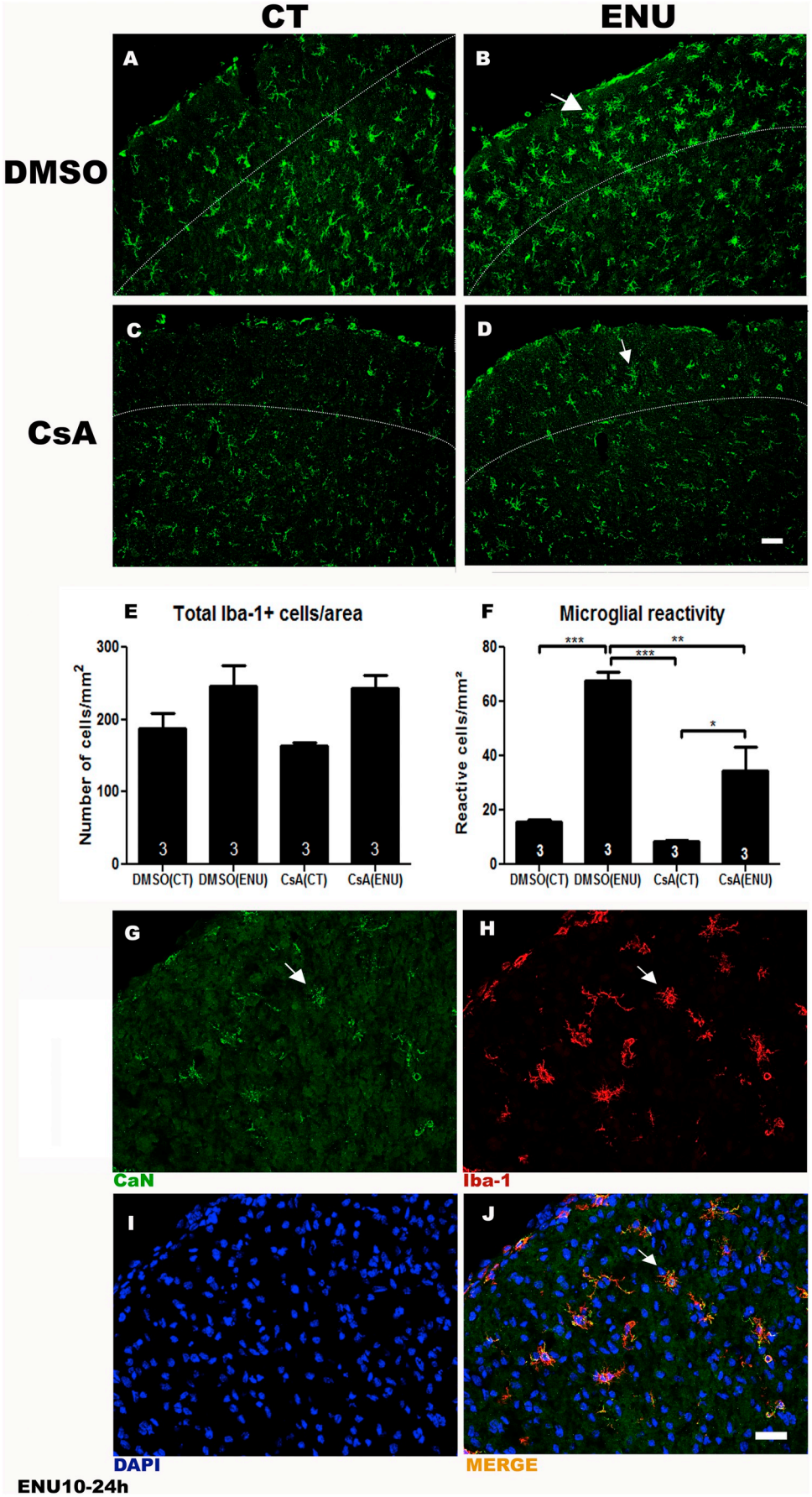

Fig. 5. Effect of an acute systemic treatment with CsA on microglial reactivity 24 h after a ME at PND10 and co-expression of CaN and Iba-1 markers. Iba-1 immunoreactivity in the SC of enucleated animals at PND10 (24 h survival) after an acute systemic treatment with either vehicle or CsA. Left side photomicrographs (CT) show the internal control SC (on the same side of the enucleated eye) (a). Right side photomicrographs (ENU) show the SC contralateral to a monocular enucleation at PND 10 (b). Notice that 24 h after a monocular eye enucleation of the contralateral SC (ENU), DMSO treated animals display more Iba-1 labeled cells than the control side (CT). An acute systemic treatment with CsA results in a marked reduction of Iba-1 immunolabeled cells in both the CT and ENU sides of the SC (c,d). Notice that in the DMSO treated group, a high intensity of fluorescence is associated with an amoeboid morphology (arrow), especially in the uppermost visual layers of the ENU SC (dashed line) (a,b). On the other hand, Iba-1 immunoreactivity of CsA treated animals is less intense and cells display a more ramified morphology (arrow) (d). Scale bar marks 100 µm. Quantification of cell densities revealed no significant differences on the total number of microglial cells (e) but revealed significant differences of reactive cells between DMSO and CsA groups (f). CaN (green) (g) co-localizes with Iba-1 (red) (h), especially in amoeboid phenotype cells (arrow). DAPI in blue (i). Notice that all photomicrographs represent a part of enucleated SC, 24 h after ME, revealing intense microglia reactivity with increased CaN expression (arrow) (j). Scale bar marks 50 µm. ANOVA, post-hoc Tukey test. n of each group is expressed on bars. Quantification was obtained by at least 3 different experiments for each group * = $p < 0,05$; ** = $p < 0,01$; *** = $p < 0,001$. (For interpretation of the references to colour in this figure legend, the reader is referred to the web version of this article.)

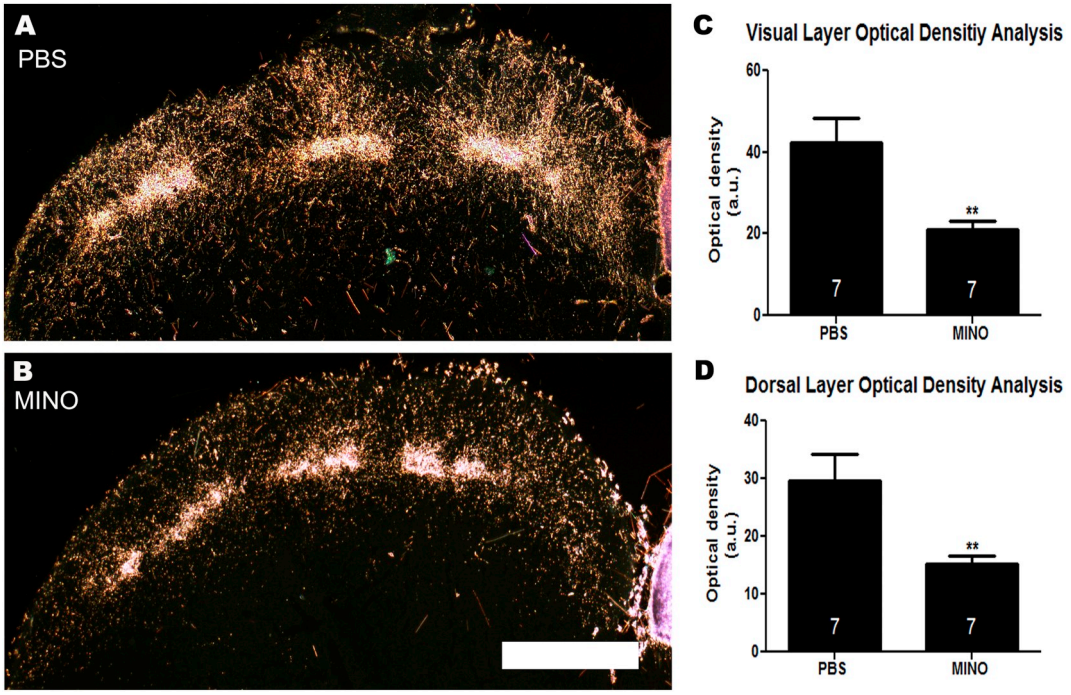

Fig. 6. Acute systemic treatment with MINO inhibts axon plasticity of the intact ipsilateral pathway induced by a monocular enucleation at PND10: Dark-field photomicrographs reveals the distribution of anterograde labeling of the ipsilateral retinocollicular pathway 24 h after a ME. The PBS treated group displays an intense sprouting of ipsilaterally projecting retinocollicular axons that spread throughout the collicular visual layers (a). On the other hand, the MINO treated group has a reduced plastic response with most of terminal labeling still confined to the clusters distributed along the ventral border of the SGS (b). Analysis of the mean optical density of either the total visual layers of the SC (c) or the dorsal SGS (d) confirm the reduction of plasticity of retinocollicular axons after an acute treatment (a single dose of minocycline 3 h after a monocular enucleation). Unpaired student's t-test. n of each group is expressed on bars. Quantification was obtained by at least 3 different experiments for each group * = $p < 0,05$; ** = $p < 0,01$; *** = $p < 0,001$. Scale bar marks 200 μm.

afferents to the contralateral dorsal lateral geniculate nucleus (dLGN) and SC and induces a reactive axonal sprouting from ipsilaterally projecting axons originating form the intact eye (Godement et al., 1980; Reese, 1986; Toldi et al., 1996). Most studies that investigated aberrant projections induced by monocular enucleation in distinct animal models studied the influence of early postnatal lesions and the interpretation of the aberrant sprouting was generally based on the reduction of synapse elimination (Chalupa and Henderson, 1980; Finlay et al., 1979; Jeffery and Thompson, 1986; Woo et al., 1985). In the present work we performed ME at PND 10 when retinotectal topography has already been formed and most of synaptic elimination has already occurred. Indeed, we observed, confirming previous observations (Serfaty et al., 2005), a very rapid and robust sprouting of the intact eye's uncrossed fibers 24 h after ME at PND10 strongly suggesting that we are observing axonal sprouting, rather than, a reduction in synapse/axonal elimination. Moreover, since the plastic rearrangement is observed from 24 h up to one year post lesion (Fig. 2C–F) it seems likely that such plasticity implies in the formation of functional synapses that would compensate for the loss of the contralateral eye's input. Such plasticity might also be present in other converging pathways, such as corticocollicular axons (Tan and Harvey, 1997).

4.2. A transient microglial activation is necessary for plasticity

In general, disturbances of CNS homeostasis (e.g. infection, trauma, ischemia, neurodegenerative diseases or altered neuronal activity) evokes, in microglial population, a rapid morphological shift to an amoeboid phenotype associated to changes in gene expression, leading to an activation state, secreting inflammatory cytokines and chemokines, followed by an astrocytic response (Kettenmann et al., 2011; Liu et al., 2011). Following a monocular enucleation in adult rodents, microglial reactivity occurs quickly after denervation and precedes astrogliosis mainly in contra- but also in ipsilateral subcortical structures, including the LGN and SC (Gonzalez et al., 2006; Hernandes and Britto, 2014; Wilms and Bahr, 1995). Rao and Lund have shown that following a monocular enucleation both MHC class I and class II antigens are expressed within 1 or 2 days postlesion by cells showing the morphological characteristics of microglia (Rao and Lund, 1993). The expression of those antigens was found along the optic pathways and within the brainstem centers to which optic axons project, suggesting that the reactive plasticity of the intact ipsilateral pathway may involve not only local microglial activation in the SC, but also the activation of microglial cells along the visual pathways.

In the present study we observed a peak of amoeboid microglia 24 h after ME with a layer-specific distribution in the SC that is correlated with a robust sprouting of intact axons suggesting a temporal correlation between compensatory axonal sprouting and microglia activation induced by a lesion. The rapid increase of reactive microglia might be a result of a local phenotype shift of resident microglia and/or local proliferation in response to acute denervation. Indeed, it has been shown that facial nerve injury results in a retrograde neuronal reaction with activation of the peri-neuronal microglia around the injured nucleus of the facial nucleus (Banati, 2003). Similarly, a lesion to the sciatic nerve is followed by microglial activation not only in the spinal cord, but also in remote areas of projection of the gracile nucleus receiving ipsilateral ascending afferents of the affected sciatic nerve (Banati, 2003). In the present study, no significant difference was observed in the total number of microglial cells (ameboid and ramified phenotypes – Fig. 3L). Therefore, the data support the hypothesis of a local phenotypic shift in response to molecular signals from the lesioned axons.

The pharmacological inhibition of microglia with CsA and minocyline, showed no difference on Iba-1content on western blot analysis 24 h after ME (Supplementary Fig. 3), although we did observe morphological changes in immunofluorescence analysis in the same time interval (Figs. 5, 6). This discrepancy could be explained by the layer-

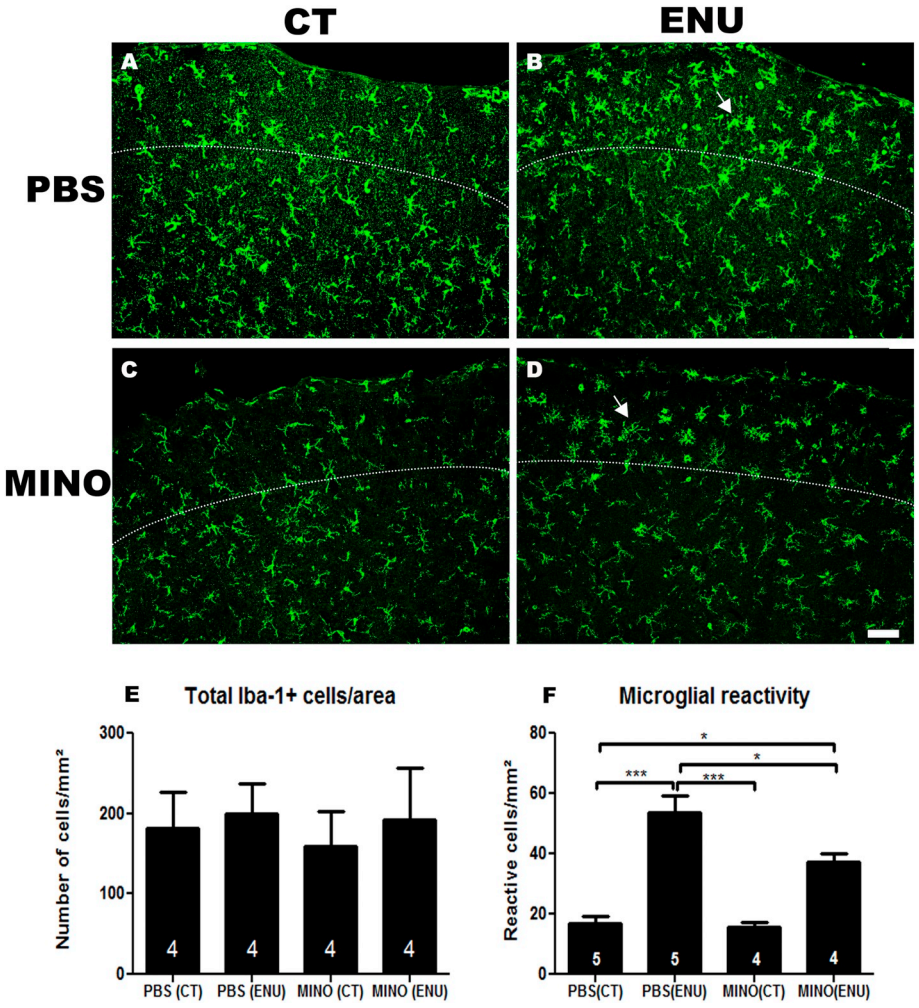

Fig. 7. Effect of an acute systemic treatment with MINO on microglial reactivity 24 h after a ME at PND10. Iba-1 immunoreactivity in the SC of enucleated animals at PND10 (24 h survival) after an acute systemic treatment with either vehicle or MINO. Left side photomicrographs (CT) show the internal control SC (on the same side of the enucleated eye) (a). Right side photomicrographs (ENU) show the SC contralateral to a monocular enucleation at PND 10 (b). 24 h after a ME, the contralateral SC (ENU) of PBS treated animals display more Iba-1 labeled cells than the control side (CT). An acute systemic treatment with MINO results in a marked reduction of Iba-1 immunolabeled cells in both the CT and ENU sides of the SC (c,d). Notice that in PBS treated animals a high intensity of fluorescence is associated with an amoeboid morphology (arrow) (b), especially in the uppermost visual layers of the ENU SC (dashed line). On the other hand, Iba-1 immunoreactivity of MINO treated animals is less intense and cells display a ramified morphology (arrow) (d). Quantification of cell densities revealed no significant differences on total number of microglia (e), but revealed significant differences of reactive cells/mm^2 between MINO and CsA groups (f). ANOVA, post-hoc Tukey test. The n of each group is expressed on bars. Quantification was obtained by at least 3 different experiments for each group * = p < 0,05; *** = p < 0,001. Scale bar marks 100 μm.

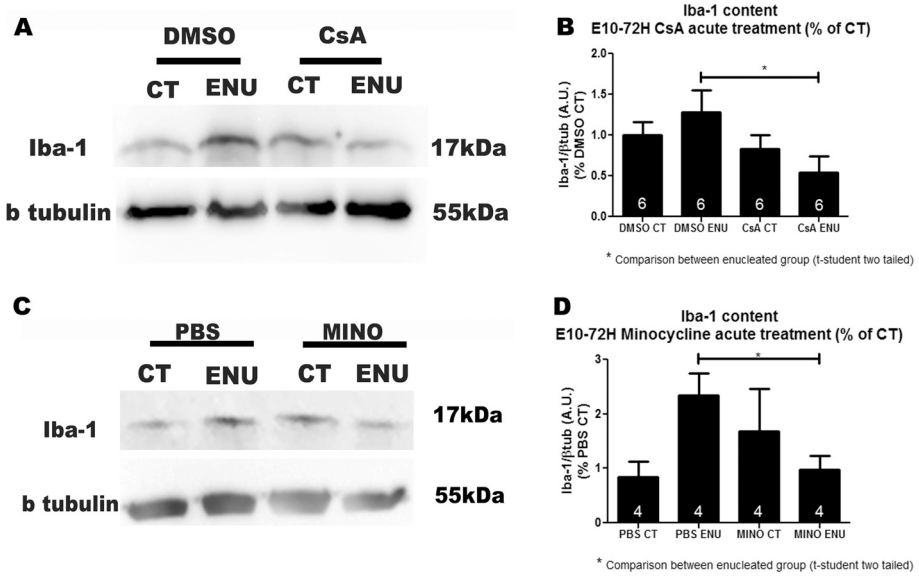

Fig. 8. Effect of acute systemic treatment with CsA and Minocycline on Iba-1 content in the SC after a ME at PND10: Western blot analysis revealed a significant reduction of Iba-1 content after an acute systemic treatment with CsA (a) and MINO (c), 72 h after enucleation at DPN10. A band of 17 kDa shows a decrease of (ENU) CsA and (ENU) MINO when compared to their respective vehicle controls. The comparison between enucleated groups revealed a significant decrease of Iba-1 content by both treatments (b, d). Unpaired student's t-test (two-tailed). The n of each group is expressed on bars. Quantification was obtained by at least 3 different experiments for each group * = p < 0,05; ** = p < 0,01; *** = p < 0,001.

specific distribution of microglial cells observed in the immunofluorescence analysis with a regional increase of amoeboid cells in the upper SGS visual layers of the SC, 24 h after the lesion, while only at 72 h post lesion we observed an increase in microglial cells in visual and non-visual layers of the SC (Fig. 3). Furthermore, it is important to notice that western blot samples were taken from the whole collicular layers including visual and non-visual layers that could mask subtle changes in Iba-1 content. Therefore western blot samples taken 24 h post-lesion did not detect significant changes while experiments at 72 h post lesion were able to reveal an increase in total Iba-1 (Fig. 3N, O) a finding in keeping with a subsequent phase of microglial proliferation or macrophage invasion of the denervated superior colliculus (London

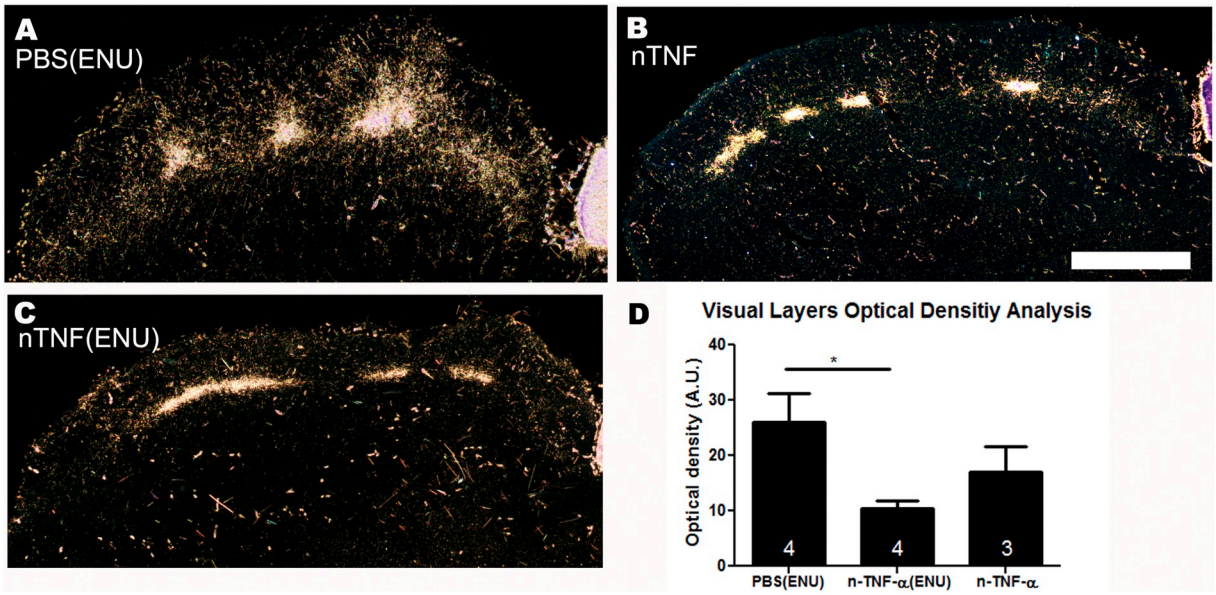

Fig. 9. Effect of the local treatment with nTNF-α antibody on the plasticity of intact axons after a monocular enucleation at PND10: Dark-field photomicrographs reveals the distribution of anterograde labeling of the ipsilateral retinocollicular pathway 24 h after a ME in animals treated with nTNF-α ELVAX implants (PND7-PND11). the group that received a PBS loaded Elvax showed a normal axonal sprouting observed in the ipsilateral retinocollicular pathway after a contralateral eye enucleation at PND10 (a). nTNF-α ELVAX implant in a non-lesioned experimental condition used as a control showed no difference to the normal developmental pattern of terminal labeling observed at PND10 (b) (see Fig. 2a, for comparison). Anterograde labeling of retinal axons in ELVAX implant loaded with nTNF-α after a ME shows a marked blockade of axon sprouting (c). ANOVA, post-hoc Dunnett's analysis of the mean optical density of the collicular visual layers area confirm the blockade of lesion-induced plasticity after a local treatment with nTNF-α. The n of each group is expressed on bars (d). Quantification was obtained by at least 3 different experiments for each group. * = $p < 0,05$. Scale bar marks 100 μm.

et al., 2013).

We must consider the possibility of two different events in the temporal course of microglial reactivity following a central lesion: the microglial polarization to M1-type in the immediate, early stages, followed by an M2-type phenotype that could exert different roles on neuroplastic responses of intact axons after a ME. At present, the mechanisms regulating microglial polarity are not clearly understood, but it has been shown that minocycline can selectively inhibit microglia polarization to a proinflammatory state in a model of amyotrophic lateral sclerosis (Kobayashi et al., 2013) and even induce an M2 polarization in an ischemia-reperfusion model of retinal degeneration (Ahmed et al., 2017). The data presented in this study do not allow to discriminate between microglial polarization, further investigation is required to answer what type of microglia is the responsible for triggering and maintaining a lesion-induced neuroplasticity.

A structural shift from ramified to amoeboid microglial phenotype in response to a CNS injury results from a reprogramming that changes not only the morphology, but also its proliferative state, the release of pro-inflammatory mediators and increase of immunomodulatory antigens on its surface (Weinstein et al., 2010). The fast microglial activation temporally correlated to structural axonal plasticity, 24 h after ME, raises the hypothesis that ipsilateral axons from the intact eye respond to the cytokines secreted by activated microglia. Furthermore, one week after the lesion, microglial profile returns to the branched, non-reactive form corroborating the hypothesis that microglia activation induced by ME would act as a trigger of the plastic changes on intact axons in the CNS. In accordance to our results, a recent work by Janz and Illing observed that the unilateral sensory ablation of the cochlear nucleus promotes microglial activation 1 day after the injury and that 7 days later, during the reinnervation phase, the number of microglial cells increase and exhibit a branched phenotype juxtaposed to neurons and terminals expressing GAP-43, a protein related to neuronal remodeling (Janz and Illing, 2014). The increase of phosphorylated GAP-43 expression in the denervated superior colliculus have also been demonstrated by our group after ME (Mendonca et al., 2010).

In a recent paper Weinhard and colleagues suggest that microglial cells are involved not only in the selective partial phagocytosis of presynaptic structures, but also in the plasticity of postsynaptic spine head filopodia (Weinhard et al., 2018). In keeping with those findings, the present study propose that microglial activation also triggers an active reorganization of presynaptic terminals in a lesion environment, as demonstrated by the anterograde axon tracing experiments. Previous studies have evidenced the capacity of reactive astrocytes in facilitating synaptogenesis and neurite outgrowth at the lesioned side by the release of trophic factors (Kawaja and Gage, 1991; Xia et al., 2002). On the other hand, once activated, astrocytes form a glial scar which encapsulate the lesion core from the healthy CNS areas (Burda and Sofroniew, 2014). The chondroitin sulfate proteoglycan NG2, a component of the glial scar was correlated with the post-lesional sprouting response in the rat fascia dentata following unilateral entorhinal deafferentation that could define boundaries for growing axons (Dehn et al., 2006). Besides, ablation of scar-forming astrocytes in a forebain stab injury presented an increase in local neurite outgrowth revealing its role in restricting nerve fiber growth after injury (Bush et al., 1999). In our model, astrocytes could be involved in de novo synapse formation and stabilization local circuits (Araque et al., 1999). In keeping with those observations, we describe that the rapid plasticity after a ME is stable after a one-year survival (Fig. 2F).

4.3. Inflammation and neuroplasticity: possible mechanisms

Two major pathways are involved in microglial reactivity: the Ca2+/CaN/NFAT pathway and the NFkB pathway. Once in the nucleus, NFATs and NFκB interact with distinct DNA binding elements to drive the expression of multiple cytokines. Following a lesion, microglia can migrate to a lesion site or herd of infectious invaders, trigger innate defense mechanisms like phagocytosis and release proinflammatory compounds to restore homeostasis (Furman and Norris, 2014; Nagamoto-Combs and Combs, 2010). In the present study we demonstrated that amoeboid microglia expresses CaN and that CsA (Lewis,

2001; Timmerman et al., 1996), concomitantly prevented both the amoeboid microglia profile and the axonal reactive sprouting. Similar results were found with another microglia inhibitor, minocycline. The pharmacological treatment with these drugs have been commonly used to prevent microglial activation, proliferation and production of proinflammatory mediators through inhibition of nuclear factor kappa B (NFkB) translocation to the nucleus (Henry et al., 2008; Tikka et al., 2001). Many studies have reported the prevention of microglial activation and the reduction of pro-inflammatory mediators such as cytokines, Cyclooxygenase-2 and induced nitric oxide synthase (iNOS) with minocycline (Tikka and Koistinaho, 2001; Yrjanheikki et al., 1999). A neuroprotective effect of CaN inhibitors has been reported in a model of focal transient brain ischemia. Either CsA or FK506 were able to reduce both microglial immunostaining for biotinylated isolectin IB4, and the levels of proinflammatory cytokines (IL -1β and TNF-α) induced by injury (Kaminska et al., 2004). Although we have used in the present study a non-isogenic strain of rats, it noteworthy to mention that different genetic backgrounds present in different strains of rodents may result in different immunological activation and different cellular responses to lesions and to immunosuppressants (Cui et al., 2007; Kigerl et al., 2006).

Uchino et al. have demonstrated that CsA ameliorates mitochondrial damage in ischemic conditions (Uchino et al., 2003), and thus acts as a neuroprotective agent. In the present study we show that under a lesion condition that induces an extensive anterograde degeneration, calcineurin co-localizes with microglial cells. In this scenario, it seems that a certain amount of neuronal degeneration induced by a monocular enucleation would be necessary to trigger microglial activation and regenerative responses from the intact eye's axons. In the same line of reasoning, the blockade of NOS activity by cyclosporine might impair an inflammatory response necessary for axonal plasticity (Diaz-Ruiz et al., 2005).

The present results cannot rule out an indirect effect of the systemic treatment with CsA or minocycline on T cells, since those cells may be involved in the modulation of microglial cells in a lesion environment (Lu et al., 2010). Furthermore, we believe that our biological model induces an innate immune response that might recruit macrophages and a crosstalk with another immunocompetent cells.

An alternative explanation of the present results would be the direct blockade of axonal outgrowth induced by immunosuppressants. Indeed, Graef et al. (2003) reported that mice deficient in calcineurin-NFAT signaling were unable to respond to neurotrophins or netrin-1 with efficient axonal outgrowth during embryonic development. Thus, it seems that immunosuppressants used in the present study may have a direct effect on the blockade of axon outgrowth. However, in a paper of Trindade et al. (2011), CsA administered in a non-lesioned rat during normal development of the rat visual pathways, produced sprouting of visual axons. This has been attributed to a blockade of long-term depression and a resulting shift toward a long-term potentiation status of visual synapses, which would drive axonal sprouting. In the present study, we present evidence that a monocular enucleation induces plasticity of the intact pathway which is co-temporal with microglial activation. CsA and Minocycline reduced microglial activation as demonstrated by immunofluorescence and western blot experiments, and a local administration of a neutralizing anti-TNFα antibody was able to reproduce the results of reduced axon sprouting after a unilateral ME. New experiments must be conducted to test whether the present data may result from a direct neuronal effect of immunosuppressants or an indirect effect through a microglial – cytokine pathway.

Ngu et al., 2007 suggested that a full accumulation of microglia is required for the usual sprouting and regeneration of damaged axons in the leech CNS (Ngu et al., 2007). Accordingly, Bechmann and Nitsch, 2000 observed that functional and morphological changes in microglia, followed by astrocytic modifications accompanies the sprouting and synaptogenesis of denervated dendrites in hippocampal terminals after a lesion at the entorhinal cortex (Bechmann and Nitsch, 2000). Recently, Baizer and colleagues investigated if reactive microglia plays a role in facilitating plastic reorganization after acoustic trauma on auditory system showing a close geographic overlap between the degenerating fibers and activated microglia (Baizer et al., 2015).

Reactive M1-type microglia produce and secrete a range of molecules necessary to support the mechanisms by which reactive cells can mediate lesion-induced plasticity of intact neuronal circuitry. Acute lesions in the CNS promote the release of a variety of proinflammatory cytokines by M1-type microglia and astrocytes, like TNF-α, Il-1β and Il-6 (London et al., 2013). And, some evidence has been ascribing a role for pro-inflammatory cytokines in lesion-induced plasticity by acting on the regulation of specific axonal reorganization and stimulating growth factors release. In a traumatic brain injury model, Oshima et al., 2009 brought evidence for a TNF-α involvement in neuroanatomical plasticity and functional recovery showing that TNF-α knockout mice lacked collateral sprouting of the unlesioned corticospinal tract when compared to wild-type mice (Oshima et al., 2009). It also has been shown that the use of TNF-α neutralizing antibody abolishes axonal regeneration after an optic nerve crush (Kreutz et al., 2004). In the present study we showed that blocking either microglial activation or TNF-α with a neutralizing antibody disrupts a compensatory local circuitry remodeling in the visual system suggesting a role of inflammation on local plasticity.

In conclusion, the present study provided evidence that a lesion during early postnatal development triggers microglial activation and cytokine secretion which in turn promotes a rapid and conspicuous plasticity of an intact axonal population. Since plasticity in human infants also has a rapid compensatory outcome (Mikellidou et al., 2017) the understanding the molecular mechanisms that allow this rapid plasticity may be an important step to modulate functional recovery in pathological conditions in the adult central nervous system. The present results may also be important to the control of maladaptive plasticity that may disturb neural circuits in neuropsychiatric disorders.

Supplementary data to this article can be found online at https://doi.org/10.1016/j.expneurol.2018.10.002.

Acknowledgements

We thank to Ms. Maria da Conceição Paiva Silva, Maria Leite Eduardo Pontes and Pedro Medina (PhD) for technical support; We also thank to Mr. Arnaldo de Sá Geraldo for animal care. This work was supported by grants from the Brazilian National Research Council (CNPq), Research Foundation of the State of Rio de Janeiro (FAPERJ), INCT/NIM, FOCEM/COF03/11 and CAPES.

Conflict of interest

The authors declare no competing financial interests.

References

Ahmed, A., Wang, L.L., Abdelmaksoud, S., Aboelgheit, A., Saeed, S., Zhang, C.L., 2017. Minocycline modulates microglia polarization in ischemia-reperfusion model of retinal degeneration and induces neuroprotection. Sci. Rep. 7, 14065.

Araque, A., Parpura, V., Sanzgiri, R.P., Haydon, P.G., 1999. Tripartite synapses: glia, the unacknowledged partner. Trends Neurosci. 22, 208–215.

Baizer, J.S., Wong, K.M., Manohar, S., Hayes, S.H., Ding, D., Dingman, R., Salvi, R.J., 2015. Effects of acoustic trauma on the auditory system of the rat: The role of microglia. Neuroscience 303, 299–311.

Banati, R.B., 2003. Neuropathological imaging: in vivo detection of glial activation as a measure of disease and adaptive change in the brain. Br. Med. Bull. 65, 121–131.

Baumgartel, K., Genoux, D., Welzl, H., Tweedie-Cullen, R.Y., Koshibu, K., Livingstone-Zatchej, M., Mamie, C., Mansuy, I.M., 2008. Control of the establishment of aversive memory by calcineurin and Zif268. Nat. Neurosci. 11, 572–578.

Bechmann, I., Nitsch, R., 1997. Astrocytes and microglial cells incorporate degenerating fibers following entorhinal lesion: a light, confocal, and electron microscopical study using a phagocytosis-dependent labeling technique. Glia 20, 145–154.

Bechmann, I., Nitsch, R., 2000. Involvement of non-neuronal cells in entorhinal-hippocampal reorganization following lesions. Ann. N. Y. Acad. Sci. 911, 192–206.

Berardi, N., Pizzorusso, T., Maffei, L., 2000. Critical periods during sensory development.

Curr. Opin. Neurobiol. 10, 138–145.
Burda, J.E., Sofroniew, M.V., 2014. Reactive gliosis and the multicellular response to CNS damage and disease. Neuron 81, 229–248.
Bush, T.G., Puvanachandra, N., Horner, C.H., Polito, A., Ostenfeld, T., Svendsen, C.N., Mucke, L., Johnson, M.H., Sofroniew, M.V., 1999. Leukocyte infiltration, neuronal degeneration, and neurite outgrowth after ablation of scar-forming, reactive astrocytes in adult transgenic mice. Neuron 23, 297–308.
Chalupa, L.M., Henderson, Z., 1980. Monocular enucleation in adult hamsters induces functional changes in the remaining ipsilateral retinotectal projection. Brain Res. 192, 249–254.
Cui, Q., Hodgetts, S.I., Hu, Y., Luo, J.M., Harvey, A.R., 2007. Strain-specific differences in the effects of cyclosporin A and FK506 on the survival and regeneration of axotomized retinal ganglion cells in adult rats. Neuroscience 146, 986–999.
Dehn, D., Burbach, G.J., Schafer, R., Deller, T., 2006. NG2 upregulation in the denervated rat fascia dentata following unilateral entorhinal cortex lesion. Glia 53, 491–500.
Diaz-Ruiz, A., Vergara, P., Perez-Severiano, F., Segovia, J., Guizar-Sahagun, G., Ibarra, A., Rios, C., 2005. Cyclosporin-A inhibits constitutive nitric oxide synthase activity and neuronal and endothelial nitric oxide synthase expressions after spinal cord injury in rats. Neurochem. Res. 30, 245–251.
Finlay, B.L., Wilson, K.G., Schneider, G.E., 1979. Anomalous ipsilateral retinotectal projections in Syrian hamsters with early lesions: topography and functional capacity. J. Comp. Neurol. 183, 721–740.
Frost, D.O., Schneider, G.E., 1979. Plasticity of retinofugal projections after partial lesions of the retina in newborn Syrian hamsters. J. Comp. Neurol. 185, 517–567.
Furman, J.L., Norris, C.M., 2014. Calcineurin and glial signaling: neuroinflammation and beyond. J. Neuroinflammation 11, 158.
Godement, P., Saillour, P., Imbert, M., 1980. The ipsilateral optic pathway to the dorsal lateral geniculate nucleus and superior colliculus in mice with prenatal or postnatal loss of one eye. J. Comp. Neurol. 190, 611–626.
Gonzalez, D., Satriotomo, I., Miki, T., Lee, K.Y., Yokoyama, T., Touge, T., Matsumoto, Y., Li, H.P., Kuriyama, S., Takeuchi, Y., 2006. Changes of parvalbumin immunoreactive neurons and GFAP immunoreactive astrocytes in the rat lateral geniculate nucleus following monocular enucleation. Neurosci. Lett. 395, 149–154.
Graef, I.A., Wang, F., Charron, F., Chen, L., Neilson, J., Tessier-Lavigne, M., Crabtree, G.R., 2003. Neurotrophins and netrins require calcineurin/NFAT signaling to stimulate outgrowth of embryonic axons. Cell 113, 657–670.
Hanson, E.S., Reese, B.E., 1993. Rapid plastic response following early retinal lesions in rats. Brain Res. Dev. Brain Res. 73, 293–298.
Henry, C.J., Huang, Y., Wynne, A., Hanke, M., Himler, J., Bailey, M.T., Sheridan, J.F., Godbout, J.P., 2008. Minocycline attenuates lipopolysaccharide (LPS)-induced neuroinflammation, sickness behavior, and anhedonia. J. Neuroinflammation 5, 15.
Hernandes, M.S., Britto, L.R., 2014. Inflammatory responses in the rat superior colliculus after eye enucleation. Brain Res. Bull. 101 (1–6).
Janz, P., Illing, R.B., 2014. A role for microglial cells in reshaping neuronal circuitry of the adult rat auditory brainstem after its sensory deafferentation. J. Neurosci. Res. 92, 432–445.
Jeffery, G., Thompson, I.D., 1986. The effects of prenatal and neonatal monocular enucleation on visual topography in the uncrossed retinal pathway to the rat superior colliculus. Exp. Brain Res. 63, 351–363.
Kaminska, B., Gaweda-Walerych, K., Zawadzka, M., 2004. Molecular mechanisms of neuroprotective action of immunosuppressants—facts and hypotheses. J. Cell. Mol. Med. 8, 45–58.
Kaur, C., Rathnasamy, G., Ling, E.A., 2017. Biology of microglia in the developing brain. J. Neuropathol. Exp. Neurol. 76, 736–753.
Kawaja, M.D., Gage, F.H., 1991. Reactive astrocytes are substrates for the growth of adult CNS axons in the presence of elevated levels of nerve growth factor. Neuron 7, 1019–1030.
Kettenmann, H., Hanisch, U.K., Noda, M., Verkhratsky, A., 2011. Physiology of microglia. Physiol. Rev. 91, 461–553.
Kigerl, K.A., McGaughy, V.M., Popovich, P.G., 2006. Comparative analysis of lesion development and intraspinal inflammation in four strains of mice following spinal contusion injury. J. Comp. Neurol. 494, 578–594.
Kobayashi, K., Imagama, S., Ohgomori, T., Hirano, K., Uchimura, K., Sakamoto, K., Hirakawa, A., Takeuchi, H., Suzumura, A., Ishiguro, N., Kadomatsu, K., 2013. Minocycline selectively inhibits M1 polarization of microglia. Cell Death Dis. 4, e525.
Kreutz, M.R., Weise, J., Dieterich, D.C., Kreutz, M., Balczarek, P., Bockers, T.M., Wittkowski, W., Gundelfinger, E.D., Sabel, B.A., 2004. Rearrangement of the retinocollicular projection after partial optic nerve crush in the adult rat. Eur. J. Neurosci. 19, 247–257.
Levelt, C.N., Hubener, M., 2012. Critical-period plasticity in the visual cortex. Annu. Rev. Neurosci. 35, 309–330.
Lewis, R.S., 2001. Calcium signaling mechanisms in T lymphocytes. Annu. Rev. Immunol. 19, 497–521.
Liu, W., Tang, Y., Feng, J., 2011. Cross talk between activation of microglia and astrocytes in pathological conditions in the central nervous system. Life Sci. 89, 141–146.
London, A., Cohen, M., Schwartz, M., 2013. Microglia and monocyte-derived macrophages: functionally distinct populations that act in concert in CNS plasticity and repair. Front. Cell. Neurosci. 7, 34.
Lu, H.Z., Wang, Y.X., Zhou, J.S., Wang, F.C., Hu, J.G., 2010. Cyclosporin A increases recovery after spinal cord injury but does not improve myelination by oligodendrocyte progenitor cell transplantation. BMC Neurosci. 11, 127.
Lund, R.D., Land, P.W., Boles, J., 1980. Normal and abnormal uncrossed retinotectal pathways in rats: an HRP study in adults. J. Comp. Neurol. 189, 711–720.
Mendonca, H.R., Araujo, S.E., Gomes, A.L., Sholl-Franco, A., da Cunha Faria Melibeu, A., Serfaty, C.A., Campello-Costa, P., 2010. Expression of GAP-43 during development and after monocular enucleation in the rat superior colliculus. Neurosci. Lett. 477, 23–27.
Mesulam, M.M., 1978. Tetramethyl benzidine for horseradish peroxidase neurohistochemistry: a non-carcinogenic blue reaction product with superior sensitivity for visualizing neural afferents and efferents. J. Histochem. Cytochem. 26, 106–117.
Mikellidou, K., Arrighi, R., Aghakhanyan, G., Tinelli, F., Frijia, F., Crespi, S., De Masi, F., Montanaro, D., Morrone, M.C., 2017. Plasticity of the human visual brain after an early cortical lesion. Neuropsychologia. https://doi.org/10.1016/j.neuropsychologia.2017.10.033. (Oct 31, pii: S0028-3932(17)30409-8, Epub ahead of print).
Mulkey, R.M., Endo, S., Shenolikar, S., Malenka, R.C., 1994. Involvement of a calcineurin/inhibitor-1 phosphatase cascade in hippocampal long-term depression. Nature 369, 486–488.
Nagamoto-Combs, K., Combs, C.K., 2010. Microglial phenotype is regulated by activity of the transcription factor, NFAT (nuclear factor of activated T cells). J. Neurosci. 30, 9641–9646.
Ngu, E.M., Sahley, C.L., Muller, K.J., 2007. Reduced axon sprouting after treatment that diminishes microglia accumulation at lesions in the leech CNS. J. Comp. Neurol. 503, 101–109.
Nys, J., Aerts, J., Ytebrouck, E., Vreysen, S., Laeremans, A., Arckens, L., 2014. The cross-modal aspect of mouse visual cortex plasticity induced by monocular enucleation is age dependent. J. Comp. Neurol. 522, 950–970.
Nys, J., Scheyltjens, I., Arckens, L., 2015. Visual system plasticity in mammals: the story of monocular enucleation-induced vision loss. Front. Syst. Neurosci. 9, 60.
Oliveira-Silva, P., Jurgilas, P.B., Trindade, P., Campello-Costa, P., Perales, J., Savino, W., Serfaty, C.A., 2007. Matrix metalloproteinase-9 is involved in the development and plasticity of retinotectal projections in rats. Neuroimmunomodulation 14, 144–149.
Oshima, T., Lee, S., Sato, A., Oda, S., Hirasawa, H., Yamashita, T., 2009. TNF-alpha contributes to axonal sprouting and functional recovery following traumatic brain injury. Brain Res. 1290, 102–110.
Rao, K., Lund, R.D., 1993. Optic nerve degeneration induces the expression of MHC antigens in the rat visual system. J. Comp. Neurol. 336, 613–627.
Reese, B.E., 1986. The topography of expanded uncrossed retinal projections following neonatal enucleation of one eye: differing effects in dorsal lateral geniculate nucleus and superior colliculus. J. Comp. Neurol. 250, 8–32.
Serfaty, C.A., Linden, R., 1991. Evidence that the relative densities of afferents from both eyes control laminar distribution and binocular segregation of retinotectal projections in rats. Brain Res. Dev. Brain Res. 60, 9–17.
Serfaty, C.A., Linden, R., 1994. Development of abnormal lamination and binocular segregation in the retinotectal pathways of the rat. Brain Res. Dev. Brain Res. 82, 35–44.
Serfaty, C.A., Campello-Costa, P., Linden, R., 2005. Rapid and long-term plasticity in the neonatal and adult retinotectal pathways following a retinal lesion. Brain Res. Bull. 66, 128–134.
Shiratori, M., Tozaki-Saitoh, H., Yoshitake, M., Tsuda, M., Inoue, K., 2010. P2X7 receptor activation induces CXCL2 production in microglia through NFAT and PKC/MAPK pathways. J. Neurochem. 114, 810–819.
Smith, A.L., Cordery, P.M., Thompson, I.D., 1995. Manufacture and release characteristics of Elvax polymers containing glutamate receptor antagonists. J. Neurosci. Methods 60, 211–217.
Steeves, J.K., Gonzalez, E.G., Steinbach, M.J., 2008. Vision with one eye: a review of visual function following unilateral enucleation. Spat. Vis. 21, 509–529.
Tan, M.M., Harvey, A.R., 1997. A comparison of postlesion growth of retinotectal and corticotectal axons after superior colliculus transections in neonatal rats. J. Comp. Neurol. 386, 681–699.
Tikka, T.M., Koistinaho, J.E., 2001. Minocycline provides neuroprotection against N-methyl-D-aspartate neurotoxicity by inhibiting microglia. J. Immunol. 166, 7527–7533.
Tikka, T., Fiebich, B.L., Goldsteins, G., Keinanen, R., Koistinaho, J., 2001. Minocycline, a tetracycline derivative, is neuroprotective against excitotoxicity by inhibiting activation and proliferation of microglia. J. Neurosci. 21, 2580–2588.
Timmerman, L.A., Clipstone, N.A., Ho, S.N., Northrop, J.P., Crabtree, G.R., 1996. Rapid shuttling of NF-AT in discrimination of Ca2+ signals and immunosuppression. Nature 383, 837–840.
Toldi, J., Feher, O., Wolff, J.R., 1996. Neuronal plasticity induced by neonatal monocular (and binocular) enucleation. Prog. Neurobiol. 48, 191–218.
Trindade, P., Antonioli-Santos, R., Teixeira, A.C., Lanzillotta-Mattos, B., Melibeu, A.C., Campello-Costa, P., Linden, R., Serfaty, C.A., 2011. Evidence for a role of calcineurin in the development of retinocollicular fine topography. Neurosci. Lett. 487, 47–52.
Uchino, H., Ishii, N., Shibasaki, F., 2003. Calcineurin and cyclophilin D are differential targets of neuroprotection by immunosuppressants CsA and FK506 in ischemic brain damage. Acta Neurochir. Suppl. 86, 105–111.
Van Brussel, L., Gerits, A., Arckens, L., 2011. Evidence for cross-modal plasticity in adult mouse visual cortex following monocular enucleation. Cereb. Cortex 21, 2133–2146.
Weinhard, L., di Bartolomei, G., Bolasco, G., Machado, P., Schieber, N.L., Neniskyte, U., Exiga, M., Vadisiute, A., Raggioli, A., Schertel, A., Schwab, Y., Gross, C.T., 2018. Microglia remodel synapses by presynaptic trogocytosis and spine head filopodia induction. Nat. Commun. 9, 1228.
Weinstein, J.R., Koerner, I.P., Moller, T., 2010. Microglia in ischemic brain injury. Future Neurol. 5, 227–246.
Wilms, P., Bahr, M., 1995. Reactive changes in the adult rat superior colliculus after deafferentation. Restor. Neurol. Neurosci. 9, 21–34.
Woo, H.H., Jen, L.S., So, K.F., 1985. The postnatal development of retinocollicular projections in normal hamsters and in hamsters following neonatal monocular enucleation: a horseradish peroxidase tracing study. Brain Res. 352, 1–13.
Wu, Y., Dissing-Olesen, L., MacVicar, B.A., Stevens, B., 2015. Microglia: dynamic mediators of synapse development and plasticity. Trends Immunol. 36, 605–613.

Xia, X.G., Hofmann, H.D., Deller, T., Kirsch, M., 2002. Induction of STAT3 signaling in activated astrocytes and sprouting septal neurons following entorhinal cortex lesion in adult rats. Mol. Cell. Neurosci. 21, 379–392.
Yrjanheikki, J., Tikka, T., Keinanen, R., Goldsteins, G., Chan, P.H., Koistinaho, J., 1999. A tetracycline derivative, minocycline, reduces inflammation and protects against focal cerebral ischemia with a wide therapeutic window. Proc. Natl. Acad. Sci. U. S. A. 96, 13496–13500.
Zheng, L.S., Kaneko, N., Sawamoto, K., 2015. Minocycline treatment ameliorates interferon-alpha- induced neurogenic defects and depression-like behaviors in mice. Front. Cell. Neurosci. 9, 5.